Fatigue Crack Growth Rate and Intrinsic Threshold Stress Intensity

R. Sunder

Abstract In atmospheric fatigue, intrinsic threshold stress intensity, $\Delta K_{th,i}$, far from being a material constant, varies significantly. It is controlled by a certain computable, load-history sensitive, near-tip residual stress, σ*, that appears to moderate crack-tip diffusion kinetics and thereby determines $\Delta K_{th,i}$, the incremental K required for an open crack to extend by fatigue. This demands reconsideration of the relationship between near-threshold crack growth rates and applied effective stress intensity range, ΔK_{eff}. Its practical implementation requires considerations of Linear Hysteretic Fracture Mechanics (LHFM). LHFM is applied to translate applied K, to near-tip cyclic inelastic stress–strain response. The new relationships permit extension of fracture mechanics considerations to short cracks including defects in additive manufactured materials and naturally forming cracks in components over high-cycle and very high-cycle (HCF/VHCF) regimes. Most importantly, the new approach permits handling near-threshold fatigue response both under constant amplitude as well as under variable-amplitude loading, representative of actual service conditions. It also permits re-interpretation of test data obtained by the so-called cyclic *R*-curve and compression-compression pre-cracking techniques.

Keywords Intrinsic threshold stress intensity · Near-tip residual stress · Near-threshold crack growth rate

1 Introduction

d*a*/d*N versus* ΔK curves obtained using standard practices such as ASTM E647 [1] serve as vital inputs to comparative evaluation of materials in design trade-off studies, residual fatigue life analyses required to assess structural integrity, safe life and life between inspections as well as in fundamental research. The discovery of fatigue crack closure [2] and incorporation of algorithms for its estimation into standard test practice permitted correction for the stress ratio effect. A vital point on this

R. Sunder (✉)
BISS Division, ITW-India (P) Ltd, Bangalore, India
e-mail: rs@biss.in

I. A. Parinov et al. (eds.), *Physics and Mechanics of New Materials and Their Applications*, Springer Proceedings in Materials 10,
https://doi.org/10.1007/978-3-030-76481-4_30

curve is ΔK_{th}, the threshold stress intensity range. Its estimation and interpretation remain controversial. This parameter is extremely crucial, particularly to applications involving extended endurance and long periods between inspections, i.e., to residual life estimates in HCF and VHCF regimes. Note also, that ΔK_{th} may influence crack growth rates right up to 10^{-4} mm/cycle.

Engineering applications involve naturally forming cracks that grow under increasing stress intensity. Laboratory testing for ΔK_{th} involves long cracks seeing load shedding. It obviously does not replicate conditions of practical interest. Long crack ΔK_{th} may not apply to naturally forming short cracks that are too short to see the consequences of certain 'extrinsic' factors [3]. Observed variations in laboratory estimates of ΔK_{th} as a function K_{max} or stress ratio, R, are typically attributed to these 'extrinsic' factors including fatigue crack closure due to plasticity, crack wake roughness and debris formation [3–5]. Implicit in such understanding is the assumption that 'intrinsic' threshold stress intensity is a material constant equal to a certain $\Delta K_{th,eff}$ (that is devoid of the main extrinsic component, namely, crack closure). The actual break-up of ΔK_{th} into its two supposed constituents has remained an enigma, given the lack of credible means to define, let alone, determine *either* of the two. On the premise that the lowest possible ΔK_{th} would represent a certain intrinsic property, different methods have been exercised in attempts to bridge the gap between laboratory test data and engineering application involving naturally forming cracks. The compression pre-cracking method is one of them [6, 7] and it is backed by numerical computations of crack closure as influenced by the process [8]. The so-called 'Cyclic *R*-Curve' is another method [9, 10]. Both these methods follow from the consideration, that by inducing reversed yield at the crack initiator, the effective notch root stress ratio even under applied compression-compression loading will turn tensile, leading to closure-free conditions under subsequent tensile stress ratio. A much simpler method to resolve the issue has been suggested that assumes that ΔK_{th} values obtained under high applied stress ratio will be associated with closure free conditions and therefore represent intrinsic component of ΔK_{th} [3]. Indeed, ΔK_{th} has been shown to progressively decrease with increasing applied stress ratio and K_{max} [11–13]. However, it remains unclear, whether it eventually does plateau in support of the crucial assumption behind the method. After all, common to all these approaches is the presumption of intrinsic threshold stress intensity as a material constant.

The so called 'two parameter approach' may appear to be by far the simplest LEFM interpretation of crack growth rate all the way down to threshold [14–17]. According to this approach, crack growth rate uniquely relates to a given combination of K_{max} and ΔK. As K_{max} approaches K_c, crack growth rate will obviously accelerate due to the increase of the quasi-static component. In the Paris Regime, the K_{max} effect can be traced to crack closure. And for reasons that are forthcoming, near-threshold crack growth rates are in addition, sensitive to K_{max} due to environmental action. In each of these stages, the very nature of the relationship between da/dN and the combination of K_{max} and ΔK will be different, being associated with vastly different mechanisms. Clearly, the two-parameter approach presents a rather simplistic picture

of an extremely interesting, but complex phenomenon. A picture, that is rendered even more complex under random load history associated with engineering application.

Finally, engineering applications involve service load history that is seldom similar to constant amplitude conditions prescribed by standard testing practices such as ASTM E647. It is generally assumed that one or more of the load interaction models will handle the difference between the two. However, available computer software in industrial use ignores the effect of variable amplitude loading on fatigue thresholds. This restricts their potential usefulness to residual fatigue lives of the order of tens, or at best, a few hundred thousand load cycles. The current study describes the framework to render laboratory crack growth rate data over their entire range, right from threshold to fracture in a manner, that suits engineering application as well as serves the purpose of future research. Its focus is on intrinsic threshold stress intensity, $\Delta K_{th,i}$ and near-threshold fatigue crack growth rates.

The next section explains why atmospheric $\Delta K_{th,i}$, cannot be a material constant and identifies a computable parameter, in the form of near-tip residual stress, σ^*, to which $\Delta K_{th,i}$ has been found to be uniquely related [18, 19].[1] The envelope of σ^* variation under both constant amplitude as well as variable amplitude loading, including the partial cases that represent cyclic *R*-curve and compression—compression loading conditions are described. This is followed by listing of $\Delta K_{th,i}$ *versus* σ^* relationships for a variety of materials obtained in previous work. New crack growth rate data on Ti-6Al-4 V obtained from similar threshold tests are collated with data obtained at higher growth rates to describe a new equation for fatigue crack growth rate that may be more suitable for engineering application than currently available representations. The paper concludes with recommendations for future work related to both research as well as engineering application.

2 Intrinsic Threshold for Atmospheric Fatigue Crack Growth

A vast body of irrefutable fractographic evidence obtained under specially designed programmed load sequences confirms, that near-threshold crack growth rates exhibit significant load sequence sensitivity that cannot be explained by 'extrinsic' factors such as crack closure [20]. This effect recedes to vanishing proportions as growth rate increases into the Paris Regime. Early work revealed that the phenomenon does not appear to exist in high vacuum [21, 22]. This prompted the Brittle Micro Fracture (BMF) theory of near-threshold crack extension, whereby the crack tip suffers Mode I micro-fracture by surface embrittlement from hydrogen in moisture at room temperature and oxidation at elevated temperature [23]. Such 'embrittlement' has been shown to be associated with highly localized slip [24, 25], that would imply

[1] Both references describe details of the testing practice to determine intrinsic threshold. However, in [18], it is referred to as ΔK_{th}, while we now refer to it as K_{th} in order to differentiate it from the notation used in the literature that represents ΔK_{th} as the sum of intrinsic and extrinsic components.

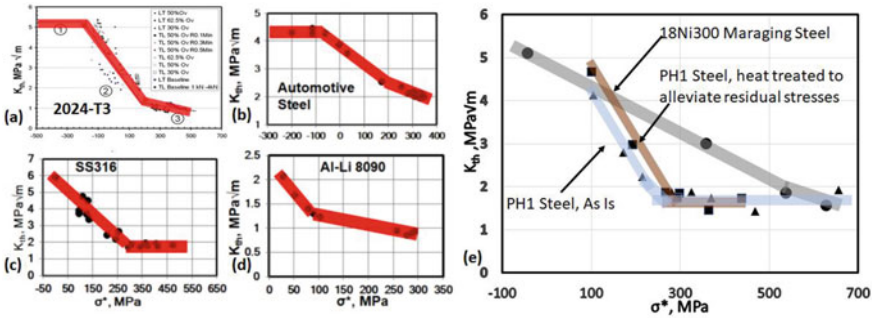

Fig. 1 Intrinsic threshold stress intensity, $\Delta K_{th,i}$, from experiments on 2024-T3 [18], automotive steel, stainless steel SS 316 and Al-Li alloy 8090 [19], and, from 3D printed high strength stainless steel, PH1 and 3D printed maraging steel 18Ni300 [27]

Mode II micro fracture. Therefore, by 'brittle' the connotation is merely about localized accelerated crack extension. Note that in the context of this work, whether it is by Mode I or II would be immaterial. Research leading up to this new understanding of variable amplitude fatigue is reviewed in [26].

If closure-free near-threshold crack growth rates are load sequence sensitive, it follows that the intrinsic component of ΔK_{th} cannot be treated as a material constant. If, however, one can relate the intrinsic component to a certain near-tip stress at the commencement of the rising load half-cycle, one can search for a relationship between them. An experimental procedure was developed to characterize intrinsic (closure free) component $\Delta K_{th,i}$ over a wide range of highly controlled and computable near-tip residual stress conditions (see Fig. 1). It was initially validated on 2024-T3 Al-alloy [18], then fine-tuned and demonstrated on a variety of materials [19] including additive manufactured materials [27].

The new experimental procedure utilizes the consequences of near-tip stress-strain hysteresis to 'set' controlled values of a certain near-tip residual stress, σ^*, through periodic application of precision controlled periodic overload/underload sequences, while at the same time decreasing ΔK with crack extension, with $P_{max} = \text{const}$, until threshold conditions conforming to 10^{-7} mm/cycle are reached. Test conditions may also include 'no overload' conditions, as the means to impose higher tensile values of σ^*. The magnitude of tensile overload is restricted to preclude the possibility of crack closure, whose absence is independently confirmed per ASTM E647. Also, crack extension during the periodic overloads constitutes a negligible fraction of baseline crack growth. The resultant threshold ΔK denoted as $\Delta K_{th,i}$ qualifies as 'intrinsic'. The absence of extrinsic component is confirmed by ensuring that K_{min} registered at threshold is well in excess of K_{op} measurement from unloading compliance made with most unconservative settings.

A fully automated test procedure permits determination of the $\Delta K_{th,i}$ *versus* σ^* relationship from a limited number of test coupons [18, 19]. As shown in Figs. 1a–e, test data from a variety of materials tested suggest a unique relationship between

$\Delta K_{th,i}$ and σ^* [18, 19, 27]. The wide range of possible cycle-sequence sensitive variation in $\Delta K_{th,i}$ points to its potential in determining residual fatigue life under service loading conditions in the HCF/VHCF range. These findings underscore limitations of prevailing standard testing practice.

It is important to note, that near-tip residual stress, σ^*, is sensitive to cyclic inelastic response well within the *cyclic* plastic zone, virtually, a crack-tip response. It is not synonymous and in fact, has little in common with 'residual stress' inferred by the well-known Wheeler [28] and Willenborg [29] crack growth retardation models that refer to the compressive residual stress caused by the stretched *monotonic* plastic zone after a tensile overload. Also, it is unrelated to the distributed residual stress that can occur by material processing [30, 31]. These 'macroscopic' residual stress distributions will affect crack closure as the crack wake will develop within their region of influence. However, the crack tip stress response will be the consequence of superposed action of such residual stress combined with that of actual cycle-by-cycle loading. This is illustrated by the $\Delta K_{th,i}$ *versus* σ^* relationships seen for AM specimens from PH1 steel, that were tested with and without heat treatment to remove residual stress (Fig. 1e). We can see a small but noticeable parallel shift in the relationship, but at higher σ^*, the two data sets merge into a flat (almost constant value), suggesting that AM-related residual stress in the material had little effect on lowest $\Delta K_{th,i}$. This may be the consequence of 'flattening out' of the monotonic near-tip stress *versus* K-curve, or, due to a certain 'saturation' in the effect of σ^* on $\Delta K_{th,i}$. Interestingly, a similar flattening of response at the lower bound is also seen in test data from the other stainless steel, SS 316 that was tested (Fig. 1c).

3 Near-Tip Stress Response and Intrinsic Threshold Stress Intensity, $\Delta K_{th,i}$

The connection between near-threshold fatigue crack growth and crack-tip diffusion kinetics has been highlighted in early work [32, 33]. The unique relationship between $\Delta K_{th,i}$ and σ^* underscores the obvious influence of instantaneous near-tip stress on diffusion kinetics, and consequently of the effect of K_{max} and particularly, of load history, two key aspects overlooked in early work that have a crucial bearing on engineering application.

Consideration of stress very close to the crack tip requires what may be referred to as a Linear Hysteretic Fracture Mechanics or LHFM approach in order to account for cycle-sequence sensitivity of near-tip stress to applied K-history. Equations associated with Linear Elastic Fracture Mechanics (LEFM) ignore near-tip cyclic inelastic response. LHFM overcomes this shortcoming by describing near-tip cyclic stress-strain hysteretic response even if K-values may conform to Linear-Elastic considerations. In the process, near-tip local *stress* history can be rendered as a function of applied stress intensity history given by equations whose description is forthcoming.

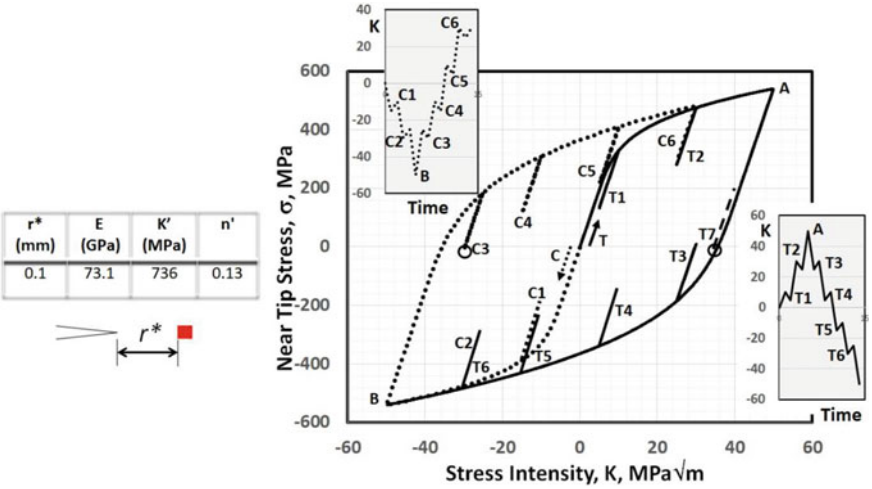

Fig. 2 Linear Hysteretic Fracture Mechanics (LHFM) representation of near-tip stress response to a complex tension-compression applied stress-intensity history. Computations made assuming fully open crack and using the constants as listed in table and (1)–(3). Variation in minimum near-tip stress in embedded cycles, σ^* should be viewed against associated variation in $\Delta K_{\text{th,i}}$ in Fig. 1a

Rendering σ^* at $K_{\min}$ as a unique function of K-history leaves *strain* response irrelevant to near-threshold fatigue even if it may retain its 'mechanistic' significance from considerations of crack closure, crack-tip blunting, etc.

Figure 2 explains the framework connecting cyclic stress–strain properties, applied load history, near-tip stress response to the applied load history including σ^* at the commencement of embedded load cycles of near-threshold magnitude and the experimentally established relationship between σ^* and intrinsic threshold stress intensity, $\Delta K_{\text{th,i}}$. The data and calculations are for 2024-T3 Al-alloy, but the same framework would be applicable for any other metallic material exhibiting strain hardening properties. The figure shows variation of near-tip stress, σ, computed for two sequences of applied stress intensity, K, for the case of a fully open fatigue crack and at a distance r^*. It is assumed that the crack wake will not close even in compression, a situation that is generally attempted to be reproduced in tests with compression—compression pre-cracking [6, 7] and in cyclic R-curve experiments [9, 10]. Near-tip response is plotted for two applied K-sequences. One sequence commenced in the tensile direction, while the other marked with the dotted line, did so in the compressive direction. The two sequences include a tensile and compressive overload marked as A and B respectively. These together form an envelope of near-tip stress response that effectively determines potential variation of σ^* for any given position of an embedded near-threshold load cycle. The material constants shown in the figure and the $\Delta K_{\text{th,i}}$ *versus* σ^* data points were obtained on 5 mm thick C(T) specimens cut from 2024-T3 [18]. These, together with the three equations below were adequate to compute the graph of σ *versus* K sequence shown:

$$K_1 = \sqrt{2\pi r^* E\sigma_1[\frac{\sigma_1}{E} + \left(\frac{\sigma_1}{K'}\right)^{\frac{1}{n'}}]} \tag{1}$$

$$K_1 - K_2 = \sqrt{2\pi r^* E(\sigma_1 - \sigma_2)[\frac{\sigma_1 - \sigma_2}{E} + 2\left(\frac{\sigma_1 - \sigma_2}{2K'}\right)^{\frac{1}{n'}}]} \tag{2}$$

$$K_3 - K_2 = \sqrt{2\pi r^* E(\sigma_3 - \sigma_2)[\frac{\sigma_3 - \sigma_2}{E} + 2\left(\frac{\sigma_3 - \sigma_2}{2K'}\right)^{\frac{1}{n'}}]} \tag{3}$$

where K_1 represents starting K-excursion from zero and following the monotonic material response, while K_2 and K_3 are the subsequent applied K-values assumed to be following the cyclic stress-strain response, associated with reversed strain and σ_1, σ_2, σ_3, are the associated near-tip stresses, E is Young's modulus, K' is the cyclic strength coefficient, n' is the cyclic strain hardening exponent and r^* is the distance from the crack tip at which local stress, σ is computed.

Note that each equation represents an excursion, whose sign would need to be inverted in the case of initial compressive excursion (the dotted line in Fig. 2). The solution of (1) determines σ_1. Similarly, solving (2) determines σ_2, while σ_3 is determined by solving (3).

The interruptions T1–T6 and C1–C6 are of equal magnitude and set to 5 MPa·m$^{1/2}$ to match the highest $\Delta K_{th,i}$ seen in the $\Delta K_{th,i}$ versus σ^* relationship for this material (Fig. 1a). The σ^* value corresponds to the minimum K-value in each of the 5 MPa·m$^{1/2}$ excursions seen. Three sets of near-threshold cycles have such minima at −30, −15, 5 and 25 MPa·m$^{1/2}$, respectively. Of these, σ^* for two, namely, C1, C2 can be computed from (1) alone. For T1–T6, σ^* requires solution of (1), (2). Estimation of σ^* for C3–C6 requires solution of (1)–(3).

The computed σ^* values are suggestive of the corresponding $\Delta K_{th,i}$ value as seen from the $\Delta K_{th,i}$ *versus* σ^* plot in Fig. 1a. The relationship between $\Delta K_{th,i}$ and σ^* being unique, *it does not matter,* what was the associated applied stress intensity. What mattered, was the LHFM-driven near-tip stress response to the applied K-sequence as estimated from (1)–(3). Note however, that the computations shown are assuming $r^* = 0.1$ mm. At this distance from the crack tip, elastic unloading over 5 MPa·m$^{1/2}$ induces a local stress change of approximately 100 MPa. This is about 35% less than at $r^* = 0.035$ mm that was used in [18]. Therefore, the $\Delta K_{th,i}$ *versus* σ^* relationship in the figure cannot be directly related to the σ *versus* K plot shown. There will be a horizontal shift in the $\Delta K_{th,i}$ *versus* σ^* relationship induced by the difference in σ^* due to elastic unloading and also a small vertical shift due to enhanced response to overloads A, B. Trends however, will remain unchanged.

Excursions T3–T6 will see the influence of overload A followed by the unloading to their respective minima. Likewise, C3–C6 will see the consequence of compressive overload B followed by tensile reloading.

Note that the four sets of three *identical* applied stress-intensity excursions, i.e., (C2, C3, T6), (C1, C4, T5), (T1, T4, C5), and (T2, T3, C6) will see vastly *different*

near-tip stress at the commencement of the rising load excursion. As a consequence, they will see vastly different $\Delta K_{th,i}$ values in atmospheric fatigue (refer to Fig. 1a). On the contrary, vastly *different* cycle pairs (C2, T6), (C1, T5), (C5, T1) and (C6, T2) end up with *minor deviation* in σ^* because of the manner in which their load history is different. These will therefore see correspondingly *similar* $\Delta K_{th,i}$ values. Note also, that cycles C3 and T3 are vastly different in terms of applied mean stress intensity, yet, σ^* in the two are not as vastly different as between identical applied cycles, e.g., C1, C4. These differences cannot be discerned by LEFM analysis. Application of LHFM to cycle-by-cycle stress-K analysis brings out the observed differences, with the added promise of opening up the possibility of modeling near-threshold variable amplitude fatigue crack growth.

Test conditions enforced by prevailing standard practice maintaining either stress ratio, R, or, K_{max} constant essentially restricts σ^* to a narrow band without necessarily freezing the extrinsic component. These two parameters have little bearing on thresholds experienced under load sequences of engineering importance. Compelling evidence in this regard emerges from a cursory comparison of load cycle C3 ($K_{max} = -25$ MPa·m$^{1/2}$) with a hypothetical load cycle T7 with K_{max} of 40 MPa·m$^{1/2}$. One of these cycles is in compression, the other in tension and separated by a difference of 65 MPa·m$^{1/2}$. Nevertheless, both will see the same $\Delta K_{th,i}$. If estimated ΔK_{th} for the two cycles does differ as it is quite likely to, the difference may *only* be attributable to the *extrinsic* fraction of ΔK_{th}.

The envelope formed by the near-tip stress response to tension-compression K-history is limited by the stress associated with highest overload and underload. The lower bounding curve in this case indicates the lowest possible σ^* at any given applied K_{min}. It determines σ^* for any load cycle 'standing' on the lower bound. The envelope illustrates the potential variation in σ^* depending on applied load history. Obviously, this margin will be controlled by strain hardening exponent, n', and the magnitude of extreme variations in loading. For the sequences in the figure, the margin of potential variation in σ^* for identical applied cycle in terms of K_{max} and K_{min} is of the order of 400 MPa. Judging from the $\Delta K_{th,i}$ *versus* σ^* relationship, this can induce significant load-history dependent variation in $\Delta K_{th,i}$. Thus, cycles C3, C4 will see lower $\Delta K_{th,i}$ values thanks to the compressive overload B, while cycles T3, T4 will see higher $\Delta K_{th,i}$ than cycles T1, T2, thanks to the overload A. This is a direct consequence of near-tip cyclic stress-strain hysteresis. It has nothing to do with crack closure, in fact, crack closure would inhibit such hysteretic response.

With increase in the magnitude of interruptions T1–T6, C1–C6, the minimum stresses in these cycles will approach the lower bound of the outer loop, reducing the variation in σ^* within each set. Simultaneously, as ΔK during these cycles is large enough to cause greater crack extension, closer to the Paris Regime (>10^{-4} mm/cycle), the associated mechanism change in crack extension will render any remaining variation irrelevant, and also effectively render LHFM considerations redundant.

The near-tip stress *versus* applied stress-intensity plot can assist in re-interpreting available test data to understand material response to the test procedures followed in compression-compression pre-cracking and from cyclic R-curve testing. Both these

strictly speaking, involve variable amplitude loading. In order to determine the $\Delta K_{th,i}$ fraction from ΔK_{th} estimated using these methods, one would need to model σ^* as a function of the applied load history in the course of compression-compression pre-cracking and cyclic *R*-curve testing.

4 Incorporation of $\Delta K_{th,i}$ into the Crack Growth Rate Equation

To be of value in engineering application, the crack growth rate equation should correctly describe crack extension during an applied load cycle that may vary by as much as seven orders of magnitude. The gradual transition of crack growth rates from threshold conditions to a magnitude, where threshold resistance ceases to be relevant needs to be adequately described by the crack growth rate equation. Judging from Fig. 3 and assuming fatigue crack extension occurs during the rising load half-cycle, the first point of interest in the load cycle is K_{op}. At K_{op}, the crack-tip 'does not know' by how much K will increase beyond this point. However, because σ^* is known, so is K_{th} that represents the incremental K required for the crack to extend by 10^{-7} mm. One may assume that this crack extension is the direct consequence of crack-tip surface diffusion kinetics associated with the rising magnitude of near-tip stress, combined with incremental crack-tip deformation.

$\Delta K_{th,i}$ can vary significantly in atmospheric fatigue depending on load history, K_{max}, etc. However, this being a crack-tip surface diffusion kinetics driven phenomenon, its significance will diminish with increasing contribution of crack extension by competing processes induced by the mechanics of crack tip response and associated crack growth once K exceeds K_{op}. Thus, whilst crack extension at 10^{-6} mm/cycle will be almost certainly influenced by $\Delta K_{th,i}$, it is unlikely crack extension at 10^{-3} mm/cycle will see the effect of $\Delta K_{th,i}$, irrespective, of whether $\Delta K_{th,i}$ for the given load cycle is small or large. At this point, it may not be appropriate to assume that da/dN is driven by the difference, $\Delta K_{eff} - \Delta K_{th,i}$.

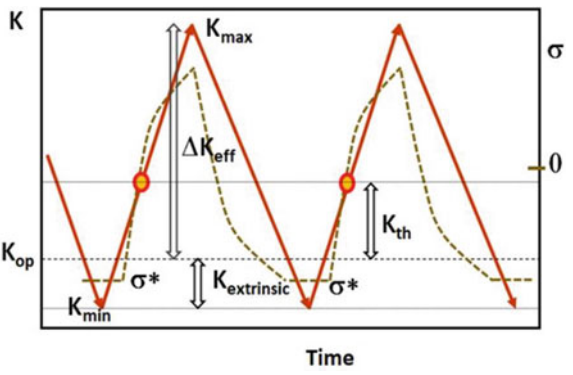

Fig. 3 Schematic variation of K and near-tip stress, σ, (broken line) in a load cycle, illustrating crack tip response to incremental loading; note flat near-tip stress response until applied incremental K exceeds extrinsic component of threshold; σ^* in turn determines the further incremental K, required for the onset of fatigue crack extension; hence there is the correlation of $\Delta K_{th,i}$ with σ^*

As K progressively increases beyond $K_{op} + \Delta K_{th,i}$, the significance of the $\Delta K_{th,i}$ component must be seen to progressively diminish as crack extension will be increasingly driven by a different mechanism altogether and increasingly sensitive only to ΔK_{eff}. This is particularly important, given the relationship between $\Delta K_{th,i}$ and σ^*. With increasing ΔK, while incremental near-tip stress towards K_{max} is attenuated by inelasticity, elastic unloading over twice the yield stress over the same ΔK will inevitably lead to lower σ^* and increasing $\Delta K_{th,i}$ over the next loading half-cycle! This is illustrated by Fig. 4a and by the broken line in Fig. 4b. Theoretically, $\Delta K_{th,i}$ in the Paris Regime will approach the highest possible values in the $\Delta K_{th,i}$ versus σ^* relationship. The receding significance of instantaneous $\Delta K_{th,i}$ in the face of rising ΔK may be accounted for by a certain effective threshold stress intensity, Δ denoted as $K_{th,eff}$ as described by the following equation valid over the range $\Delta K_{th,i} < \Delta K_{eff} < \Delta K^*_{eff}$:

$$K_{th,eff} = \Delta K_{th,i} \left[\frac{\left(\Delta K^*_{eff} - \Delta K_{eff}\right)}{\left(\Delta K^*_{eff} - \Delta K_{th,i}\right)} \right]^p \tag{4}$$

where, ΔK^*_{eff} is ΔK_{eff} associated with a growth rate of 10^{-3} mm/cycle and p is a constant, assumed for brevity to be unity. The form of this equation meets boundary conditions associated with both threshold as well as with the total disappearance of near-threshold response at $\Delta K_{eff} \geq \Delta K^*_{eff}$.

One may expect that ΔK^*_{eff}, being associated with the Paris Regime, will always exceed $\Delta K_{th,i}$. Actual value of p is likely to be determined by the competition of the two crack extension mechanisms involved. Determination of a more suitable value of p can be the subject of future work. However, judging from forthcoming empirical evidence, $p = 1$ appears reasonable.

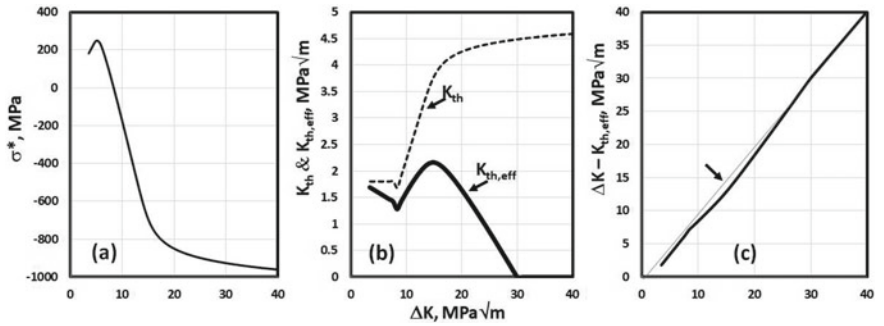

Fig. 4 Transformations of near-threshold response for Ti-6Al-4 V at $R = 0.3$: **a** computed near tip residual stress as a function of applied ΔK; **b** variation in $\Delta K_{th,i}$ with applied ΔK per (**a**) and $K_{th,eff}$ corrected for 'proximity of Paris Regime'; **c** kink indicated by arrow is due to the variation in $K_{th,eff}$. This may explain local deviation in da/dN data from expected log-linear relationship. Note that extrinsic component of ΔK_{th} is ignored *in these computations*

$\Delta K_{\text{th,i}}$ is computed as a dependent variable of ΔK_{eff} and associated $K_{\max}$ from the $\Delta K_{\text{th,i}}$ *versus* σ^* relationships as shown in Fig. 1. Under constant amplitude loading, the computed value of $\Delta K_{\text{th,i}}$ will be valid for a given stress ratio and known crack closure. Under near threshold conditions defined by the condition: $\Delta K_{\text{eff}} < \Delta K^*_{eff}$, crack growth rate will be influenced by $K_{\text{th,eff}}$. At $\Delta K_{\text{eff}} \geq \Delta K^*_{eff}$, $K_{\text{th,eff}} = 0$, i.e. at the other end, as $K_{\max}$ approaches K_c, increasing contribution of quasi-static component from local fracture by micro-void coalescence, strain localization across brittle constituents, etc. will accelerate growth. An equation that describes this entire range of growth rate may be assumed to take the form:

$$\frac{da}{dN} = C\left[\Delta K_{eff} - K_{th,eff}\right]^m \frac{1}{\left(1 - \frac{K_{max}}{K_c}\right)^q}, \Delta K_{eff} < \Delta K^*_{eff} \tag{5}$$

$$\frac{da}{dN} = C\left[\Delta K_{eff}\right]^m \frac{1}{\left(1 - \frac{K_{max}}{K_c}\right)^q}, \Delta K_{eff} \geq \Delta K^*_{eff} \tag{6}$$

where, K_c is the fracture toughness and q is a constant assumed for brevity to be unity. The correction of da/dN to account for $K_{\max} \rightarrow K_c$ is the same as that adopted widely in the literature. Equation (6) is essentially the same as (5) with the exception that $K_{\text{th,eff}} = 0$.

Note that (5) is limited to da/d$N \geq 10^{-7}$ mm/cycle. As engineering practice constantly pushes the demands on durability and residual crack growth life to higher cycle counts, $\Delta K_{\text{th,i}}$ will arguably also require reconsideration in terms of associated da/dN. For engineering purposes, one may extend $\Delta K_{\text{th,i}}$ at 10^{-7} down to 10^{-9} mm/cycle by correction of its value given the slope of da/dN curve at 10^{-7} mm/cycle.

We now proceed to summarise the procedure to determine the material constants in (5).

5 Material Constants and Validation

Obviously, a number of material constants are involved in forming an equation that attempts to describe variation of crack growth rate over seven orders of magnitude. Particularly so, when the 'origin' of the da/dN curve corresponding to threshold da/dN of 10^{-7} mm/cycle is itself highly sensitive to $\sigma^*.\sigma^*$ in turn is determined using constants that describe the cyclic stress-strain curve. Near-threshold crack growth rates will depend on $\Delta K_{\text{th,i}}$ as well as the emerging dominance of the Paris regime parameters C and m. Finally, the addition of quasi-static component from the proximity of fracture will accelerate growth rate as $K_{\max}$ approaches K_c.

Computation of near-tip stress response leading to the characterization of the $\Delta K_{\text{th,i}}$ *versus* σ^* relationship requires constants defining the cyclic stress-strain curve

of the material, namely, Young's modulus, E, cyclic strength coefficient, K', and cyclic strain hardening exponent, n' (see Fig. 2).

A realistic evaluation of the new framework involves an attempt to correlate experimental data over the entire range of associated crack growth rates, i.e., from 10^{-7} to 10^{-1} mm/cycle. Such a correlation can be assessed by plotting data in the log-log scale as $\frac{da}{dN}\left(1-\frac{K_{max}}{K_c}\right)$ against $\Delta K_{eff}-K_{th,eff}$. A good fit would be indicated by a linear fit with slope, m, and intercept C.

Experimental data obtained on Ti-6Al-4 V in the course of this data were consolidated using the above framework. All the required tests were performed at BISS Labs on a BISS 25 kN high performance servo-hydraulic test system permitting test frequency of up to 250 Hz. The tests were performed on 5 mm thick, 50 mm wide C(T) specimens, with test frequency set to 100 Hz to ensure amplitude error less than 1%. Two of the specimens were tested to determine $\Delta K_{\text{th,i}}$ values under a wide range of σ^*. The crack growth curves from these tests appear as Fig. 5.

The test procedure to characterize the $\Delta K_{\text{th,i}}$ versus σ^* relationship is described in detail elsewhere [18, 19, 27]. The sets of transient data covering a reasonably wide range of growth rate are consolidated as da/dN *versus* ΔK in Fig. 6. Given the nature of the transients involving cycling at $P_{\max}$ = const and steadily increasing $P_{\min}$ to impose receding ΔK, the stress ratio associated with individual data points invariably increases with reducing crack growth rate, reaching up to values in excess of $R = 0.8$. Also shown in Fig. 6 are data from a single constant amplitude test performed at stress ratio $R = 0.3$ and assumed to involve little or no crack closure. For the same reason, ΔK may be treated as ΔK_{eff} for these data.

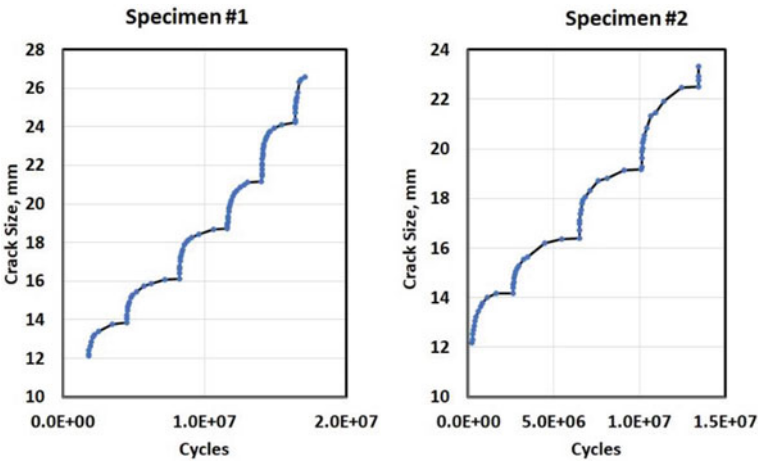

Fig. 5 Crack growth curves registered during tests on two specimens to characterize $\Delta K_{\text{th,i}}$ as a function of σ^*. Each segment on the curve corresponds to a regime of receding ΔK with $P_{\max}$ = const and possible periodic overload/underload sequence to 'set' required σ^*. Transient crack growth rate points from these curves appear as circles in Fig. 6

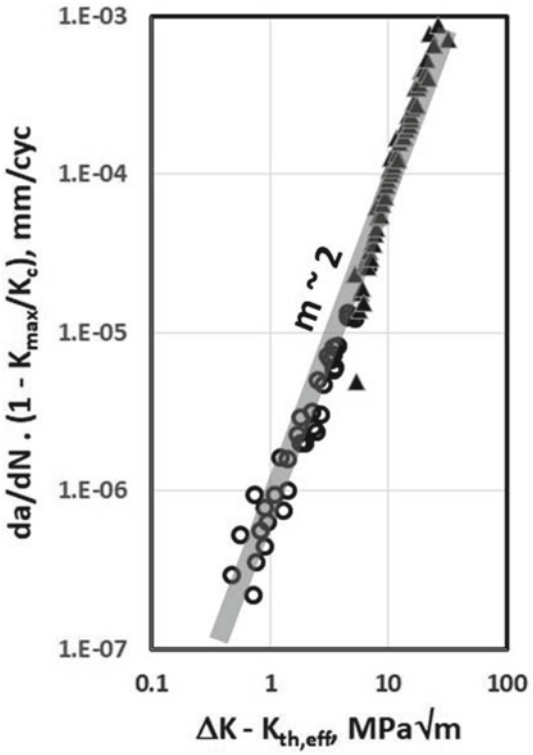

Fig. 6 Crack growth rate data from a single test on Ti-6Al-4 V at $R = 0.3$ (triangles) plotted along with transient da/dN data (circles) from the threshold tests to characterize $\Delta K_{\text{th,i}}$ *versus* σ^*; closure at $R = 0.3$ was ignored, as was in the transient data points all of which occurred at $R > 0.5$

The data in Fig. 6 are plotted as $\frac{da}{dN}\left(1 - \frac{K_{max}}{K_c}\right)$ against $\Delta K - K_{th,eff}$. Also shown in the figure is a trend line suggesting a slope $m = 2$ over the data range.

6 Discussion

The discovery of crack closure was a turning point in understanding stress ratio and load interaction effects in fatigue crack growth. Establishment of the unique relationship between $\Delta K_{\text{th,i}}$ and σ^* may serve as the next turning point by explaining why significant load interaction effects will persist even in the absence of crack closure, and why, the significance of these effects increases disproportionately into near-threshold fatigue, that dominates in the HCF and VHCF domains.

By drawing the line between propagating and non-propagating cracks, thresholds effectively determine fatigue limit. In doing so, the new understanding also provides a fundamental explanation as to why fatigue limit diminishes with mean stress, a phenomenon known (albeit unexplained) for more than 150 years from the pioneering work of Wöhler and Bauschinger [34].

The new procedure to determine the relationship between $\Delta K_{th,i}$ and σ^* suggests more conservative estimates of $\Delta K_{th,i}$ than would follow from conventional testing practice. To cite an example of consequences for engineering application to naturally forming cracks, given the estimates obtained on Ti-6Al-4 V, it would follow that the potential minimum size of cracks that can propagate at a given applied stress level would be less than half the size expected from the lowest ΔK_{th} estimates from conventional testing practice. This, given the square root dependence of K on crack size.

The $\Delta K_{th,i}$ *versus* σ^* relationship appears to lay to rest misunderstandings caused by prevailing testing practices to characterize fatigue thresholds, that resulted in attempts to relate ΔK_{th} to K_{max}, R-ratio, etc.,. Obviously, given a certain partial pressure of active species and rate of loading, the degree of BMF in a single rising load half cycle would be determined by the extent of their surface diffusion. The associated diffusion kinetics at a given temperature will be moderated by a certain instantaneous near-tip hydrostatic or biaxial stress as it increases from that, at the commencement of the rising load half cycle, i.e., from σ^*. For this reason, $\Delta K_{th,i}$ correlates with near-tip stress at the commencement of the rising half of the load cycle, rather than at K_{max}. Strictly speaking, this stress should not be referred to as 'residual' because by 'residual' one would imply stress at no load. However, the two would be synonymous, if $K_{min} \leq K_{op}$, as near-tip stress response can be assumed to cease below K_{op}.

It has for long been wrongly assumed, that by accounting for crack closure and other shielding effects, laboratory constant amplitude crack growth rate data can be extended to variable-amplitude loading. While closure does indeed go a long way in bridging the gap, its ability to do so becomes increasingly diluted in the near-threshold region leading down to threshold. This gap extends to a three order of magnitude variation in crack growth rate, where instantaneous $\Delta K_{th,i}$ comes into play. Closure can at best account for the extrinsic component of ΔK_{th}. The intrinsic component is uniquely related to near-tip residual stress, a parameter that like closure, is also sensitive to crack tip mechanics, but in ways that are very different from crack closure. Unlike crack closure, near-tip residual stress is cycle-sequence sensitive. Unlike crack closure, it can exhibit cycle-to-cycle bi-directional variation and do so, even without requiring crack extension. While crack closure is largely wake driven, near-tip stress variation requires an open crack.

The form of the modified (5) for da/dN accounts for the manner in which growth rate transits from threshold into the Paris regime. Further, the relationship between $\Delta K_{th,i}$ and σ^* combined with the treatment of $\Delta K_{th,i}$ as a cycle-sequence sensitive variable in the equation opens up the possibility of modeling variable-amplitude fatigue from its very early stages. Thus, variable-amplitude fatigue crack growth can be modeled as a consequence of the combined action of crack closure and crack-tip blunting on the one hand and on the other, by the effect of these on σ^* on a cycle-by-cycle basis. Such a 'tri mechanism' or 'TriM' model was successfully applied to model residual crack propagation lives in the range from 5 to 20 million cycles for 2024-T3 alloy under an extended duration transport aircraft load spectrum [35]. A fractographic study of the failures obtained revealed significant load sequence

sensitive variations in fatigue crack extension during the large fraction of smaller load cycles. These were adequately modeled by correcting $\Delta K_{th,i}$ over these cycles as a function of load history. There are hardly any data in the literature reflecting attempts to model residual life, exceeding even a million cycles, suggesting limitations posed by the lack of threshold data suitable for engineering application.

Unlike closure that develops early and persists throughout the crack growth process and is rather independent of the mechanisms that drive crack extension, intrinsic threshold fades into vanishing proportions as da/dN exceeds 10^{-4} mm/cycle. For this reason, both load interaction effects as well as environment related effects affected by $\Delta K_{th,i}$ will fade away with increasing growth rate. The latter was clearly brought out in early experiments by Bradshaw and Wheeler on the influence of test frequency and partial pressure of moisture on crack growth rates [36]. These highlighted the increasing effect of both test frequency and partial pressure of moisture with decreasing crack growth rate. It follows that if growth rates below the Paris regime are involved, prevailing approaches to laboratory data generation and modeling are limited in their ability to come up with residual life estimates of value to engineering practice. Moreover, given the vast difference in the physics behind crack closure and near threshold response, one cannot hope to 'fudge' the effect of the latter through distorted simulation of the former.

Load interaction effects have also been modeled by simulating mean stress variation in the cyclic plastic zone using a cumulative damage approach [37]. However, such an approach, just as also, the two-parameter approach [14] do not focus on the phenomenon in question, namely, the influence of near-tip stress on threshold response. They are faulted in wrongly assuming that the effect persists across the entire range of growth rates.

Most of fatigue life is exhausted in the early stages of fatigue crack growth. As nondestructive inspection technologies improve, smaller fatigue cracks can be detected to permit increased service life between inspections. The potential for induction of additive manufactured components in safety critical applications can benefit greatly from the ability to estimate the residual life assuming pre-existing defects associated with the 3D printing process. All these imply a rising demand for capability to estimate residual crack growth life in the HCF and VHCF regimes. Obviously, this is less likely to materialize without the ability to model $\Delta K_{th,i}$ variation along with other load interaction mechanisms such as closure. Analytical modeling of $\Delta K_{th,i}$ under variable-amplitude loading, combined with that of crack closure appears to be a potentially rewarding area of future research.

Discovery of the close connection between near-threshold fatigue crack growth behavior and near-tip residual stress raises new questions and opens new avenues in fatigue research of direct application value. An important new avenue of fundamental research is the search for an analytical connection between partial pressure of active species such as moisture in air and oxygen at high temperature, rate of loading (or frequency) and the relationship between $\Delta K_{th,i}$ and σ^*. One would expect a lateral shift in this relationship, whose model would significantly reduce the cost of future testing effort. An even more significant impact of engineering value would be the

development of engineered materials with improved resistance to surface diffusion of active species.

The new findings are also likely to impact a new interpretation of near-threshold region of sustained load cracking. Thus, it is likely that if service loading involves hold-time at an intermediate load level, one would have to consider the hysteretic variation in near-tip stress depending on whether such hold time occurs on the rising or falling half of a major load cycle.

From the standpoint of immediate application, an important question relates to the definition of r^*. In previous work, the goal was to select a value that provides the best correlation between $\Delta K_{th,i}$ and σ^*. It is not clear whether r^* thus selected will also deliver the best estimates of variable amplitude fatigue crack growth life, when cycle-by-cycle correction of $\Delta K_{th,i}$ is resorted to as a function of σ^*, computed at a given r^* for a given service load sequence. Another relates to the choice of cyclic-stress strain curve. K' and n' in this study were based on tests on smooth specimens. However, they are applied to a point ahead of the crack tip that is likely to see the effect of constraint, where K' and n' are likely to be different. Strictly speaking, r^* should be zero. However, analysis treats the crack tip to be a singularity, that in itself, is an approximation. Notwithstanding this contradiction, the consistent and reproducible relationship between $\Delta K_{th,i}$ and σ^*, seen in all the materials that were tested testifies to its uniqueness and reproducibility. It also suggests the apparent irrelevance of K_{max} and stress ratio that have served testing practice for all these years.

Finally, naturally forming small cracks will be sensitive to local phenomena as induced by microstructure such as grain size, grain boundary orientation and local mechanical property variations [38], that go beyond the scope of this study. The important question is whether such cracks will grow, or, get arrested. It now emerges, that in atmospheric fatigue, in addition to the three threshold states highlighted by Miller, instantaneous K_{th} as affected by loading conditions including load history plays a major role in controlling the fate of naturally forming small cracks that eventually determines durability.

7 Conclusions

(1). $\Delta K_{th,i}$, the intrinsic component of ΔK_{th}, is sensitive to a certain, computable, near-tip residual stress, σ^*, whose variation can be analytically described for a given load history, based on a material's cyclic-stress strain response. This enables accounting for significant load history effect on K_{th}, that hitherto appears to have been wrongly considered to be a material constant.

(2). Experiments on Ti-6Al-4 V test coupons show variations in K_{th} between 1.25 and 4.3 MPa·m$^{1/2}$, in what appears to be a unique relationship with σ^*. This trend and nature of relationship is similar to that, observed on several other materials that showed a variation up to a factor of five.

(3). An equation is proposed for crack growth rate that accounts for variations in $\Delta K_{th,i}$ in the transient region between threshold and the Paris regime. This equation appears to show good correlation of near-threshold crack growth rates obtained from tests on Ti-6Al-4 V test specimens. It can be used to account for effects of both load ratio as well as load history in engineering estimates of residual fatigue life extended into the HCF and VHCF regimes.

(4). The unique relationship between $\Delta K_{th,i}$ and σ^* appears to represent a scientific explanation for the residual stress effect on naturally forming small cracks growing in the absence of closure.

Acknowledgements The author is grateful to Air Force Research Laboratories (AFRL), WPAFB-OH, USA and University of Dayton, for the provision of Ti-6Al-4V C(T) test specimens. The tests were carefully performed by Meghanathan.

References

1. ASTM E647–15e1, *Standard Test Method for Measurement of Fatigue Crack Growth Rates* (ASTM International, West Conshohocken, PA, 2015). www.astm.org
2. W. Elber, in *Damage Tolerance in Aircraft Structures, ASTM STP 486* (ASTM International, West Conshohocken, PA, 1971), p. 230
3. R.O. Ritchie, D.L. Davidson, B.L. Boyce, J.P. Campbell, O. Roder, Fatigue Fract. Eng. Mater. Struct. **22**, 621 (1999)
4. A.K. Vasudevan, S. Suresh, Metall. Mater. Trans. A. **13**, 2271 (1982)
5. S. Suresh, G.F. Zamiski, R.O. Ritchie, Metall. Trans. A **12**, 1435 (1981)
6. J.C. Newman, J. Schneider, A. Daniel, D. McKnight, Int. J. Fatigue **27**, 1432 (2005)
7. J.C. Newman, Y. Yamada, Int. J. Fatigue **32**, 879 (2010)
8. S.W. Smith, B. R. Seshadri, J.A. Newman, in *15th International Symposium on ASTM/ESIS Symposium on Fatigue and Fracture Mechanics*, May 20–22, 2015, Anaheim, CA (2015)
9. K. Tanaka, Y. Akiniwa, Eng. Fract. Mech. **30**(6), 863 (1988)
10. J. Maierhofer, S. Kolitsch, R. Pippan, H. Gänser, M. Madia, U. Zerbst, Eng. Fract. Mech. **198**, 45 (2018)
11. L. Lawson, E.Y. Chen, M. Meshii, Int. J. Fatigue **21**, S15 (1999)
12. D.A. Taylor, *Compendium of Fatigue Thresholds and Growth Rates* (Engineering Materials Advisory Services Ltd., West Midlands, UK, 1985)
13. B.L. Boyce, R.O. Ritchie, Eng. Fract. Mech. **68**, 129 (2001)
14. A.K. Vasudevan, K. Sadananda, N. Louat, Scr. Metall. **28**, 65 (1993)
15. K.J. Miller, Int J. Fatigue **23**, S277 (2001)
16. A.K. Vasudevan, K. Sadananda, N. Louat, Mater. Sci. Eng. **A188**, 1 (1994)
17. A.K. Vasudevan, K. Sadananda, Int. J. Fatigue **21**, S263 (1999)
18. R. Sunder, Mater. Perform. Charact. (An ASTM J.) **4**(2), 105 (2015)
19. R. Sunder, R. Koraddi, C. Vishwas, Mater. Perform. Charact. J. Am. Soc. Test. Mater. (2020). https://doi.org/10.1520/MPC20190223
20. R. Sunder, Int J. Fatigue **27**, 1494 (2005)
21. R. Sunder, W.J. Porter, N.E. Ashbaugh, Fatigue Fract. Eng. Mater. Struct. **26**, 1 (2003)
22. N.E. Ashbaugh, W.J. Porter, A.H. Rosenberger, R. Sunder, in *Proceedings of the Fatigue 2002*, Stockholm, June 2–7, EMAS (2002)
23. R. Sunder, Fatigue Fract. Eng. Mater. Struct. **28**(3), 289 (2005)

24. Y. Ro, S.R. Agnew, R.P. Gangloff, Metall. Mater. Trans. **A39A**, 1449 (2008)
25. Y. Murakami, T. Kanezaki, Y. Mine, S. Matsuoka, Metall. Mater. Trans. A. **39**, 1327 (2008)
26. R. Sunder, J. ASTM Int. **9**(1), JAI103940 (2012). ASTM Special Technical Publication. **1546**, 20 (2012)
27. R. Sunder, R. Koraddi, A. Gorunov, in *Structural Integrity of Additive Manufactured Materials and Parts*, ed. by N. Shamsaei, M. Seifi (ASTM International, West Conshohocken, PA, 2020), p. 188
28. O.E. Wheeler, ASME J. Basic Eng. **94**, 181 (1972)
29. J. Willenborg, R.H. Engle, H.A. Wood, Report No. AFFDL-TM-71-1 FBR, WPAFB, OH (1971)
30. M.R. Hill, J.E. Van Dalen, M.B. Prime, Press. Vessel. Pip. Div. **6**, 251 (2011)
31. A. Diana, D.A., Lados, D. Apelian, J. Keith Donald, Int. J. Fatigue **29**, 687 (2007)
32. C.Q. Bowles, Report No. LR-270, Delft Univ. of Technology, Delft, The Netherlands (1978)
33. J. Petit, G. Henaff, C. Sarrazin-Baudoux, ASTM Spec. Tech. **1372**. American Society for Testing and Materials, West Conshohocken, PA (2000)
34. A. Anon, Engineering **4**, 160 (1867)
35. R. Sunder, in *Lecture Notes in Mechanical Engineering*, ed. by R.V. Prakash et al. (Eds.) (Springer Nature Singapore, Singapore, 2020). https://doi.org/10.1007/978-981-13-8767-8_1
36. F.J. Bradshaw, C. Wheeler, Int. J. Fract. Mech. **6**, 255 (1969)
37. S. Mikheevsky, G. Glinka, Int. J. Fatigue **31**, 1828 (2009)
38. K.J. Miller, ASTM STP 1296 Am. Soc. Test. Mater. **267** (1997)